Biochimica et Biophysica Acta 1840 (2014) 2386–2395

Contents lists available at ScienceDirect

Biochimica et Biophysica Acta

journal homepage: www.elsevier.com/locate/bbagen

Cell jamming: Collective invasion of mesenchymal tumor cells imposed by tissue confinement☆

Anna Haeger [a,1], Marina Krause [a,1], Katarina Wolf [a,1], Peter Friedl [a,b,c,*,1]

[a] Radboud Institute for Molecular Life Sciences, Department of Cell Biology, Post 283, PO Box 9101, 6500HB Nijmegen, The Netherlands
[b] UT MD Anderson Cancer Center, Genitourinary Medical Oncology-Research, Houston TX, USA
[c] Cancer Genomics Center, The Netherlands

ARTICLE INFO

Article history:
Received 4 February 2014
Received in revised form 25 March 2014
Accepted 28 March 2014
Available online 8 April 2014

Keywords:
Melanoma
Fibrosarcoma
Cell migration
Collagen matrix
Elastic modulus
Matrix metalloproteinase

ABSTRACT

Background: Cancer invasion is a multi-step process which coordinates interactions between tumor cells with mechanotransduction towards the surrounding matrix, resulting in distinct cancer invasion strategies. Defined by context, mesenchymal tumors, including melanoma and fibrosarcoma, develop either single-cell or collective invasion modes, however, the mechanical and molecular programs underlying such plasticity of mesenchymal invasion programs remain unclear.
Methods: To test how tissue anatomy determines invasion mode, spheroids of MV3 melanoma and HT1080 fibrosarcoma cells were embedded into 3D collagen matrices of varying density and stiffness and analyzed for migration type and efficacy with matrix metalloproteinase (MMP)-dependent collagen degradation enabled or pharmacologically inhibited.
Results: With increasing collagen density and dependent on proteolytic collagen breakdown and track clearance, but independent of matrix stiffness, cells switched from single-cell to collective invasion modes. Conversion to collective invasion included gain of cell-to-cell junctions, supracellular polarization and joint guidance along migration tracks.
Conclusions: The density of the extracellulair matrix (ECM) determines the invasion mode of mesenchymal tumor cells. Whereas fibrillar, high porosity ECM enables single-cell dissemination, dense matrix induces cell–cell interaction, leader–follower cell behavior and collective migration as an obligate protease-dependent process.
General significance: These findings establish plasticity of cancer invasion programs in response to ECM porosity and confinement, thereby recapitulating invasion patterns of mesenchymal tumors *in vivo*. The conversion to collective invasion with increasing ECM confinement supports the concept of cell jamming as a guiding principle for melanoma and fibrosarcoma cells into dense tissue.
This article is part of a Special Issue entitled Matrix-mediated cell behaviour and properties.
© 2014 Elsevier B.V. All rights reserved.

1. Introduction

Cancer invasion and dissemination into tissue is a multi-step process which balances mechanotransduction towards the ECM[2] with cell–cell interactions between tumor cells. Tumor cell movement may result from distinct migration strategies determined by both, molecular properties of the tumor cells as well as mechanical and signaling input from the tumor microenvironment. Mesenchymal single-cell migration results from stringent adhesion sites linked to high actomyosin-mediated traction force and the capability to proteolytically degrade or remodel ECM [1,2]. Conversely, amoeboid single-cell migration is mediated by weak cell adhesion to ECM coupled to protrusive leading edge kinetics, including filopodia or blebs, and absence of structural ECM remodeling [3]. Distinct from single-cell movement, collective cell migration depends upon intact cell–cell junctions providing mechanical and signaling connection between tumor cells for supracellular polarization and coordination [4–6]. In collagen-rich 3D ECM, collective cell migration requires an integrin-based force generation and proteolytic cleavage of ECM to generate migration tracks that accommodate the moving cell group [1,7,8]. These cell migration programs are adaptive and interconvertible in response to cell-intrinsic and stroma-derived inputs [2].

☆ This article is part of a Special Issue entitled Matrix-mediated cell behaviour and properties.

* Corresponding author at: Radboud Institute for Molecular Life Sciences, Department of Cell Biology, Post 283, PO Box 9101, 6500HB Nijmegen, The Netherlands. Tel.: +31 24 3610907.
E-mail addresses: a.haeger@ncmls.ru.nl (A. Haeger), p.friedl@ncmls.ru.nl (P. Friedl).
URL: https://www.radboudumc.nl/Research/Organisationofresearch/Departments/cellbiology (P. Friedl).
[1] Tel.: +31 24 3614329.
[2] Extracellular matrix.

http://dx.doi.org/10.1016/j.bbagen.2014.03.020
0304-4165/© 2014 Elsevier B.V. All rights reserved.

As central mechanism for the conversion from multicellular to single-cell pattern, EMT[3] leads to the downregulation of stringent E-cadherin-based cell–cell junctions which releases individually migrating cells from multicellular epithelia [9–11]. Consistently, mesenchymal tumor cells migrate individually after experimental cell dissociation and exposure to 2D and 3D *in vitro* substrates, similar to migrating fibroblasts [12,13]. However, mesenchymal cells can also develop N-cadherin-based collective migration patterns in 3D models of multicellular invasion *in vitro* and mouse models of interstitial invasion [1,7,9,14–19]. Whereas molecular mechanisms of cell–cell junction regulation and cell patterning are well established, tissue determinants for single-cell *versus* collective migration modes remain unclear.

Depending on the type of tissue microenvironment, invading tumor cells are confronted with different extracellular structures and molecular patterns which jointly determine the biomechanics of cell–matrix interaction and migration efficacy. Physical, extracellular modulators of cell migration include: confinement, based on pore-size through which the cell migrates; geometry along which the cell-body aligns, determined by ECM alignment and dimensionality (2D vs. 3D); and stiffness which, depending on the composition, flexibility, density and cross-link status of ECM components, can vary greatly between tissue types and healthy or malignant tissue [20–22].

Collagen I, the main component of ECM in interstitial tissues, determines the spatial organization and stability of connective tissues. Natural patterns of collagen topography include low-density zones consisting of thick and thin collagen bundles forming a porous meshwork of random or aligned organization, or high-density zones, composed of tightly arranged and often aligned collagen bundles with micron-scale pore size. While loose connective tissue is usually located adjacent to epithelial layers, including the dermis or gut submucosa, densely packed collagen bundles dominate the desmoplastic peritumoral stroma [17,20,23,24]. To recapitulate such heterogeneity of ECM topography and density, multi-scale approaches were developed to predict how moving cells integrate varying tissue organization by adjusting migration mode and efficacy [25].

Several types of adaptation were identified in moving cells in response to ECM heterogeneity. Contact guidance enables cells to take the path of least resistance when confronted with discontinuous environments, which supports preferential migration along ECM interfaces or aligned structures [17,25–30]. As a fundamental biomechanical determinant, deformation of the cell body and nucleus maintains individual cell movement through narrow pores of mechanically challenging environments [31,32]. To overcome tissue constraints, cell deformation is further complemented by the pericellular cleavage of ECM proteins through cell-derived MMPs,[4] which increases space for facilitated single-cell and collective cell migration [1,8,20,33–35]. In addition, pericellular functionalization of ECM is achieved by paracrine deposition of ECM components which may increase ligand density and stiffness and thereby modulate mechanocoupling during migration [2,21,25,36–38]. These cellular responses cooperate and support a repertoire of adaptation responses to cope with heterogeneous tissue organization during migration.

Depending on the experimental model, mesenchymal cells, including fibroblasts, neural crest cells, fibrosarcoma and melanoma cells, migrate either individually or as collective cell groups [1,7,12,18], however the environmental conditions enabling such diversity of migration mode are poorly understood. Using a systematic approach to modulate ECM density, stiffness and availability of MMP-dependent pericellular proteolysis, we here address how mechanical and molecular requirements govern the balance between single-cell and collective invasion of mesenchymal melanoma and fibrosarcoma cells. The data show mesenchymal patterning and migration mode as a function of matrix porosity and support proteolytic track clearance followed by cell jamming as key steps to collective mesenchymal migration in confining environments.

[3] Epithelial–mesenchymal transition.
[4] Matrix metalloproteinases.

2. Material and methods

2.1. Cell culture

Human wild-type HT1080 fibrosarcoma (ACC315; DSMZ Braunschweig) [39] and human wild-type MV3 melanoma (provided by G. van Muijen, Dept. of Pathology, RadboudUMC Nijmegen, The Netherlands) [40] cells were cultured (37°C at 5% CO_2 humidified atmosphere) in Dulbecco's Modified Eagle's Medium (DMEM; Invitrogen) supplemented with 10% FCS (Sigma-Aldrich), penicillin (100 U/ml) and streptomycin (100 μg/ml; both PAA), L-glutamine (2 mM) and sodium pyruvate (1 mM; both Invitrogen). MMP function was inhibited by the broad-spectrum inhibitor GM6001 (ilomastat; EMD Millipore) at non-toxic concentration (20 μM) [13].

2.2. 3D spheroid culture

Cells from subconfluent culture were detached with EDTA (1 mM) and trypsin (0.075%; Invitrogen), and multicellular spheroids were generated using the hanging-drop method [41]. In brief, cells were suspended in medium supplemented with methylcellulose (20%; Sigma) and incubated as droplets (25 μl) containing 7000 (MV3) or 4000 (HT1080) cells for 24 h to ensure multicellular aggregation.

For 3D culture in collagen, spheroids were washed (PBS) and mixed with collagen solution consisting of non-pepsinized rat-tail collagen (BD Biosciences/Corning) at different concentrations (2.5 mg/ml to 8.0 mg/ml). Collagen–spheroid mixtures were either incorporated into a custom chamber or pipetted as a drop-matrix and polymerized at 37°C [31]. To generate collagen lattices with both high ligand and porosity, collagen polymerization in a custom chamber was performed at low temperature (21°C) which delayed polymerization and increased both fiber caliber and pore dimensions, as described [23,31]. (For reconstituting high-density matrices, the commercially available collagen stock solution was concentrated to 12.0 mg/ml using a SpeedVac Concentrator (Savant) prior to reconstitution to a final concentration of 6.0 or 8.0 mg/ml).

Spheroid-containing collagen lattices were maintained at 37°C for 24 h (HT1080 cells) or 48 h (MV3 cells).

2.3. Time-lapse microscopy and cell tracking

Emigration from spheroid cultures in 3D fibrillar collagen was monitored at 37°C using digital time-lapse, bright-field microscopy (20×/0.30 NA air objective; Leica) connected to CCD cameras (Sentech) and Vistek software for up to 72 h at 4 min frame interval.

Cell tracking and quantification of the migration index was performed manually, using tracking plugin, area selection- and measurement tools of the Fiji/Image J software (v1.48) [42].

2.4. Confocal fluorescence microscopy and quantification of matrix porosity and 3D invasion

Spheroids in 3D collagen matrices were fixed (4% PB-buffered PFA), washed (PBS) and stained using the following reagents: mouse anti-ALCAM mAb (AZN-L50; IgG2A; Department of Tumor Immunology, Radboud Institute for Molecular Life Sciences (RIMLS), The Netherlands [43]); polyclonal rabbit anti-COL23/4C Ab (collagen I cleavage site) (Immunoglobe); secondary Alexa-Fluor-488-conjugated goat anti-rabbit or anti-mouse IgG (Invitrogen); Alexa-Fluor-488- or Alexa-Fluor-568-conjugated phalloidin (Invitrogen); DAPI (Roche). For COL23/4C staining, samples were pre-incubated with murine serum IgG (Sigma) to reduce non-specific background adsorption, followed by addition of primary antibody prior to fixation.

For multicolor detection of fluorescent spheroids inside collagen lattices, long working distance confocal microscopy was performed (Olympus FV1000 scanner; 20×/0.50 NA water immersion objective). Z-stacks were obtained at 5 μm slice intervals. Migration analysis was performed on DAPI- and phalloidin-stained spheroids using high-content epifluorescence microscopy combined with automated multi-position image acquisition and stitching (Leica DMI6000B; 20×/0.50 NA air objective; 25 μm slice interval). Maximum intensity z-projections were used to quantify the number of emigrated single cells, multicellular strands, area and length of strands and the angles between strand axis and mitotic planes using Fiji/Image J software (v1.48) [42] (Fig. S1).

Pore size measurements of cell-free fibrillar collagen were performed in custom chambers also used for 3D spheroid invasion cultures. The reflectance signal from collagen fibers was obtained by confocal scanning (Olympus FV1000; 40×/0.80 NA water immersion objective) as xy scans with 1 μm slice intervals and 30 μm z-depth from a central region of approximately 200 μm distance from the cover glass. Pore cross sections were measured from individual xz slices, as described [31].

2.5. Collagen stiffness measurement by AFM[5]

Cell-free collagen matrices (~5 μl) were reconstituted in a WillCo-dish with PDMS insert, overlaid with PBS and probed in native state by AFM using a cantilever with an attached polystyrene microsphere (10 μm diameter) on a Catalyst BioScope (Bruker) coupled to a confocal microscope (TCS SP5 II; Leica) [31]. Bead attachment, calibration, measurements and data analysis (conversion of force–distance curves into force–indentation curves (F–δ)) were performed as described [44]. Subsequently F–δ curves were fitted over the 0–0.6 nN range after baseline correction using in-house written Igor Pro 6 (WaveMetrics) algorithms kindly provided and written by Jonne Helenius (BSSE, ETH Zürich, Basel, Switzerland) and Joost te Riet (Department of Tumor Immunology, Radboud Institute for Molecular Life Sciences (RIMLS), The Netherlands) to calculate the stiffness with the Hertz model for spheres in contact with a flat surface [45]:

$$F = \frac{4E\sqrt{R_c}}{3(1-\nu^2)} \cdot \delta^{\frac{3}{2}}.$$

2.6. Statistics

Statistical analysis was performed by the two-tailed unpaired Mann–Whitney test using GraphPad Prism 5 software.

3. Results

To identify matrix requirements and molecular determinants underlying collective invasion in mesenchymal tumor cells, we here used 3D multicellular spheroid cultures of MV3 melanoma and HT1080 fibrosarcoma cells in mechanically defined 3D collagen environments of varying density. We monitored invasion mode and efficacy as well as MMP-dependent ECM remodeling.

3.1. Transition from individual to collective cell migration as a function of ECM density

3D low- to high-density fibrillar collagen scaffolds were reconstituted from rat-tail type I collagen and analyzed for porosity by 3D confocal backscatter reconstruction combined with image analysis of pore dimensions between fibers. With increasing collagen concentration matrix porosity was incrementally reduced, resulting in a median pore range between 24 μm^2 for low-density (2.5 mg/ml) and 3.5 μm^2 for high-density conditions (8.0 mg/ml) (Fig. 1A, B). This pore range is suited to accommodate an efficient single-cell migration of individualized MV3 [46] and HT1080 [31] cells in the absence of molecular interference.

To test for the impact of collagen density on migration mode, multicellular spheroids of MV3 and HT1080 cells were embedded inside 3D collagen matrices with varying density and monitored for the efficacy and type of cell invasion. Using both, bright-field time-lapse microscopy (Fig. S1A) and 3D reconstructions of fixed and stained spheroid cultures (Fig. 1C; Fig. S1B, C), the migration mode was quantified as the frequency of single-cell *versus* collective invasion pattern. Both cell types showed a significant discrimination of ECM density by invading as individual cells or loose chains without retaining cell–cell junctions in loose (2.5 to 4.0 mg/ml) and predominantly collective strands in dense fibrillar collagen (6.0 to 8.0 mg/ml) (Fig. 1C; Fig. S2A). Concurrently, increasing collagen density impeded (collective) invasion, detected as decreased number of invading cells and reduced length or area of invasion strands (Fig. S2B, C), while inducing a gradual conversion from single-cell to collective invasion as a linear function with near-exclusive collective invasion reached at pore cross sections of ~4 μm^2 (Fig. 1D).

To address whether the physical matrix porosity, rather than an altered content of collagen ligand and/or fibril thickness, controls ECM-imposed plasticity of invasion mode, 3D matrices of low porosity were generated by using high collagen concentration (8.0 mg/ml) with delayed polymerization speed at low temperature [31]. Compared with collagen matrices polymerized at 37°C, this altered polymerization regime led to lattices with nine-fold larger pores and increased fiber caliber (Fig. 1A, B). Concomitant to increased porosity, collective invasion reverted to the single-cell pattern in both cell types, reaching near-complete individual dispersion similar to low-density collagen matrices (Fig. 1C, D; Fig. S1A; Fig. S2). An unexpected second-order morphological switch could be detected when comparing both high-porosity conditions: Whereas spindle-shaped, mesenchymal invasion with clearly visible actin-fibers was predominant in low-density microfibrillar conditions (2.5 mg/ml), single cells moving into macrofibrillar porous matrix (8.0 mg/ml, 21°C) showed near-exclusive rounded morphologies without profound actin-fibers, indicative of amoeboid migration (Fig. 1C) [2,3]. Thus, irrespective of collagen ligand density, the space between fibrils controls whether mesenchymally migrating single cells resort to the collective invasion pattern.

3.2. ECM-density imposed features of collectivity: path-coordination, cell–cell junctions and polarization

While single-cell migration, including multicellular streaming, lacks long-lasting adhesive junctions between moving cells, collective migration depends upon cell–cell interactions and supracellular communication, resulting in a coordinated path structure and front-rear polarity [2,5,9]. Time-lapse analysis of cell position and path organization of collective strands invading high-density 3D collagen matrices showed a defined leader–follower behavior with a single tip-cell leading the strand as well as near-complete alignment of the migration tracks of cells composing the strand. Conversely, cells moving individually in low-density scaffolds lacked a dedicated follower behavior resulting in individualized tracks that did not, or rarely, overlapped with neighbor paths (Fig. 2A, B; Movies #1, 2) Thus, spatial confinement imposes "leader–follower" patterns and shared migration tracks.

To test whether ECM-induced alignment of migration tracks coincides with intact cell–cell junctions, invading spheroid cultures were stained for Activated Leukocyte Cell Adhesion Molecule (ALCAM/CD166), which provides homophilic cell–cell interactions and is highly expressed in MV3 and HT1080 cells (data not shown). As expected, cell–cell junctions in the spheroid-body showed a linear colocalization

[5] Atomic force microscopy.

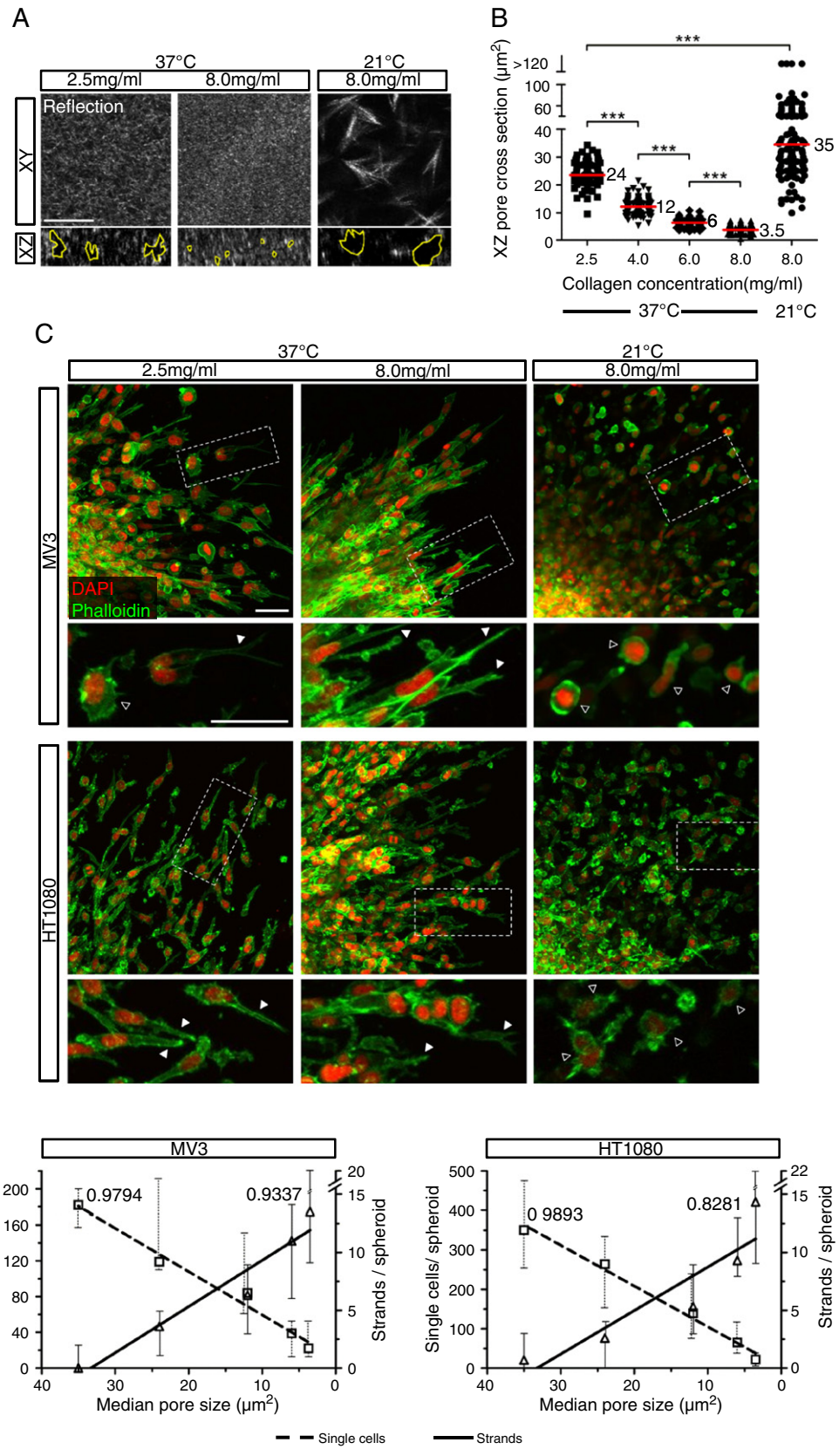

Fig. 1. Matrix-density dependent switch from individual to collective cell migration in MV3 and HT1080 cells. A) Xy and xz confocal reflectance scans of rat-tail collagen matrices of different concentrations and polymerization temperatures and B) quantification of pore cross-sections (example pores outlined in xz-scan). $P < 0.0001$ from 3 to 4 independent experiments with measurements from ~12 different locations/gel. Red horizontal line: median. C) Emigration from spheroids 24 h (HT1080) and 48 h (MV3) after embedding in collagen matrices of different densities, detected as maximum intensity projection from confocal 3D stacks. Dashed rectangles: region of detail images. Black arrowheads: roundish, amoeboid cells. White arrowheads: elongated, mesenchymal shapes. D) Migration pattern as a function of median pore area. Frequency of single-cell or collective invasion from 30 to 70 spheroids/condition (3–5 independent experiments), shown as medians and 5th/95th percentiles (whiskers) derived from Fig. S2B. Approximate cell number per strand at the end-point was 15 (MV3) and 16 (HT1080). R^2 values for regression lines are indicated in the graph. Scale bars: 10 μm (A); 50 μm (B).

of ALCAM and F-actin (Fig. 2C, region 1). Likewise, multicellular invasion strands retained linear ALCAM in colocalization with F-actin along cell–cell interactions for both, MV3 and HT1080 cells, consistent with adhesive and functional collectivity (Fig. 2C, region 2).

Functional cell–cell cooperativity is further supported by a striking alignment of mitotic plane perpendicular (= angle of ~90°) to the length-axis of invasion (Fig. 2D). Thus, spatial confinement imposes central features of collective cell migration in mesenchymal tumor cells, including joint trails, linear cell-to-cell junctions with a cortical actin layer and collective front-rear polarization.

3.3. Collagen degradation requirements for overcoming barriers in ECM-driven collective invasion

When monitored side-by-side and irrespective on cell–cell cooperativity, the net speed of invasion in both, MV3 and HT1080 cells, was delayed with increased collagen density during both, early-onset and late invasion (Fig. 3A; Fig. S1A; Movies #1, 2).

Collagenolysis mediated by MMPs is a prerequisite for *de-novo* track generation and collective invasion of tumor cells [1,26] or invasion-inducing fibroblasts [8], suggesting space restriction as a support principle for collective cell–cell cooperation. Consistent with MMP-dependent proteolytic collagen degradation and track generation, collective cell movement into high-, but not low-density collagen matrix was ablated by the broad-spectrum MMP inhibitor GM6001 (Fig. 3B, C; Fig. S3A, B). With MMPs inhibited, single-cell dissemination in low-density collagen was, however, associated with a more elongated and spindle-shaped morphology, indicating enhanced cell deformation as protease-independent rescue strategy to navigate through partly confining ECM (median pore size ~24 μm^2) (Fig. 3B, C). Despite the lack of MMP activity, time-lapse movies and F-actin staining revealed that cells in dense collagen were “trying hard” to exit the spheroid body. Especially for HT1080 cells long, F-actin positive and DAPI negative, anuclear cell protrusions extended from the spheroid and, after disruption, moved into the collagen (Fig. 3B; Fig. S3C; Movie #3). Such moving leading edges ripping apart from the main cell body followed by autonomous movements indicate high mechanical tension along the cell body, as described for single cells arrested in dense ECM [31]. Thus, proteolytic collagen breakdown is indispensable for collective invasion enforced by high-density ECM.

To directly show collagen cleavage and proteolytic track formation collagen degradation neoepitope (Col2¾C) was assessed for control and GM6001-treated samples. Pericellular collagen degradation was present along the periphery of both, single cells and collective strands with MMP activity unperturbed, and absent in the presence of GM6001 (Fig. 3D). Thus, cell extensions and migrating F-actin containing anuclear cell fragments were independent of collagen breakdown but, because of arrested position of the main cell body and nucleus, insufficient to establish MMP-independent multicellular invasion strands as a consequence of space constraints (Fig. 3B, insets).

3.4. Invasion pattern independent of matrix rigidity

In addition to porosity, altered collagen matrix density impacts mechanical properties of the migration substrate. To test whether ECM stiffness independently controls invasion patterns [36,47], the elastic modulus of collagen scaffold types associated with single-cell or collective migration was probed by AFM (Fig. 4A). Constant force input was provided and downward movement of the cantilever together with the collagen surface was registered (Fig. 4B). ECM conditions associated with single-cell dissemination showed either high (8.0 mg/ml, 21°C) or low (2.5 mg/ml, 37°C) rigidity, whereas scaffold conditions favoring collective invasion (8.0 mg/ml, 37°C) showed an intermediate stiffness level (Fig. 4C). Thus, the single-cell to collective invasion switch was a function of ECM porosity (compare Fig. 1D) but not rigidity (Fig. 4 C). This identifies matrix porosity as dominant modulator of migration plasticity.

4. Discussion

Proteolytic tracks of least resistance generated by leader cells provide 3D space and an aligned interface which accommodate multiple cell bodies and guide collective migration. The transition from single-cell to collective invasion of mesenchymal MV3 melanoma and HT1080 fibrosarcoma cells in response to strong ECM confinement thus provides wet-lab evidence for cell jamming [48] as plasticity mechanism supporting collective cell migration in 3D tissue.

To probe the mechanisms balancing single-cell *versus* collective invasion of mesenchymal cells, we here used a type I collagen-based 3D model that matches the spectrum of tissue porosity and rigidity *in vivo*. Its pore-size range (0.5 to 170 μm^2) represents the estimated space between collagen fibers *in vivo* ranging from 2 to 30 μm diameter which reflects both upper and lower limits of interstitial tissue densities and, to the lower end, reaches strong confinement near the physical limit of cell migration [17,23,31,49]. Likewise, the initial diameter of proteolytic migration tracks established by leader cells amounts to 10–20 μm which corresponds to the space between collagen interfaces *in vivo* [2,17]. The stiffness range of *in vitro* generated collagen matrices (24 to 1160 Pa) corresponds to the stiffness of diverse tissues ranging from 20 Pa (adipose tissue) to 1000 Pa (interstitial tissue and tumor stroma) [22,50–53]. Other *in vitro* models provide similar confinement and rigidity, including microchannels of defined width [47,54–56] and stiffness [47], however, due to their synthetic polymer-based organization these models preclude cell-derived space adjustments by pericellular degradation or ECM remodeling [1,21,25,57]. 3D collagen matrices thus provide a reasonably physiological model for the biomechanics and susceptibility to cell-derived physicochemical modification of *in vivo* tissues. Beyond the biology of fibrillar collagen, additional modulation of cell–cell and cell–matrix interactions likely occurs in response to additional structural and molecular complexity not included in this study, including signals from collagen subtypes, fibronectin, laminins, and proteoglycans [21,58,59]. Thus, addressing additional microenvironmental modulation of cell patterning will require the use of polymorphous multimolecular ECM models that probe additional complexity of cell invasion, including cell adaptation and decision making when confronted with tissue heterogeneities.

Whereas collective cell migration is an established feature of normal epithelia and endothelia moving as cohesive sheets or tube-like strands across or through interstitial tissue [9,38,60–62], the ability of mesenchymal cells to move collectively remains controversial [5]. The plasticity response observed here confirms that constitutively mesenchymal tumor cells may readily switch between individual and collective migration strategies, depending on spatial confinement. Similar plasticity is observed in neural crest cells during development which, after EMT, adapt a variety of migration strategies, including single-cell migration, multicellular streaming and/or collective migration modes [63–67]. Likewise, invasive mesenchymal fibrosarcoma or breast cancer cells after EMT generate single-cell or collective patterns, depending on the availability of ECM-degrading MMPs [1]. Several features identified here indicate that tissue confinement contributes to the acquisition of collective cooperativity in mesenchymal cells. These include the precise use of joint trails, the maintenance of linear cell-to-cell junctions containing ALCAM and a cortical actin layer as well as a collective front-rear polarization with leader–follower behavior [2,5,68]. Thus, by dictating a morphological pattern, plasticity of migration directly impacts intercellular communication and coordination. Beyond the here identified switch from single-cell to collective migration in mesenchymal cells, a transition from elongated, spindle-shaped to roundish, amoeboid morphologies was noted for migration conditions of highest porosity. 3D ECM ligand density and porosity variation thus likely impose such single-cell plasticity response by regulating cell adhesion strength

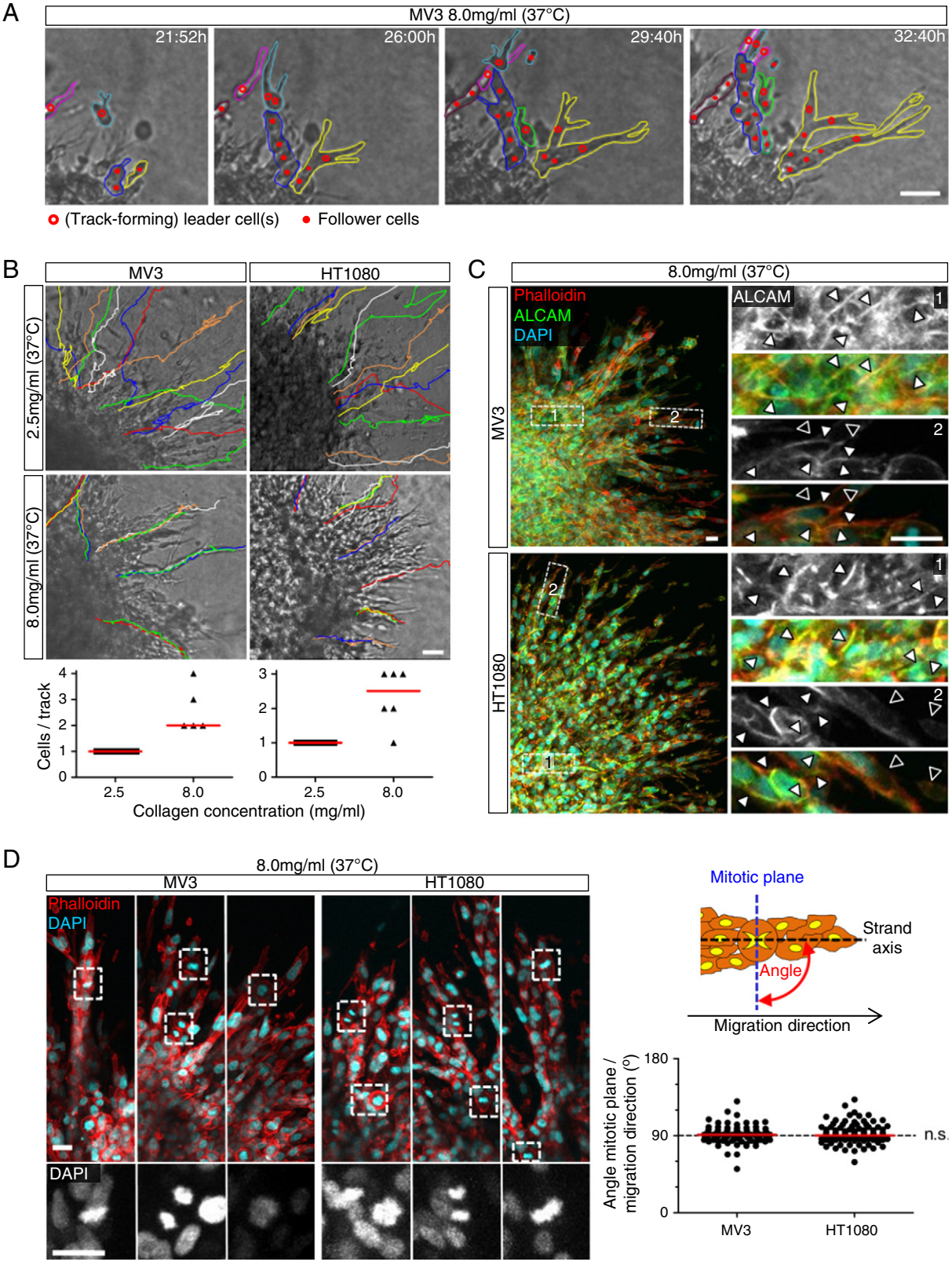

Fig. 2. Multicellular path coordination, cell interactivity and polarity in MV3 and HT1080 cells with ECM confinement. A) Early-onset collective MV3 cell strands guided by individual leader cells. Frames taken from Movie #1 with individual invasion zones outlined in color. B) Positional alignment of cell tracks in fibrillar collagen of high (8.0 mg/ml) but not low density (2.5 mg/ml). 2D paths were taken from the center of individual cells and represented in orthotopic position. For quantification, cells were defined as following the same track if tracks showed a ± 10 μm overlay for at least 50% of the track length. C) F-actin and ALCAM-positive cell–cell contacts during collective invasion into dense collagen matrix. White arrowheads: linear ALCAM distribution along cell–cell junctions. Black arrowheads: relative ALCAM deficiency in the periphery of leader and follower cells. D) Orientation of mitotic planes in collective invasion strands. Angles were measured between longitudinal strand axis and mitotic plane axis as obtained from 3D confocal reconstructions (left panels) and displayed (right panel) (~110 mitotic figures from ~40 independent spheroids). Scale bars: 50 μm (A, B); 25 μm (C, D). Red horizontal line: median.

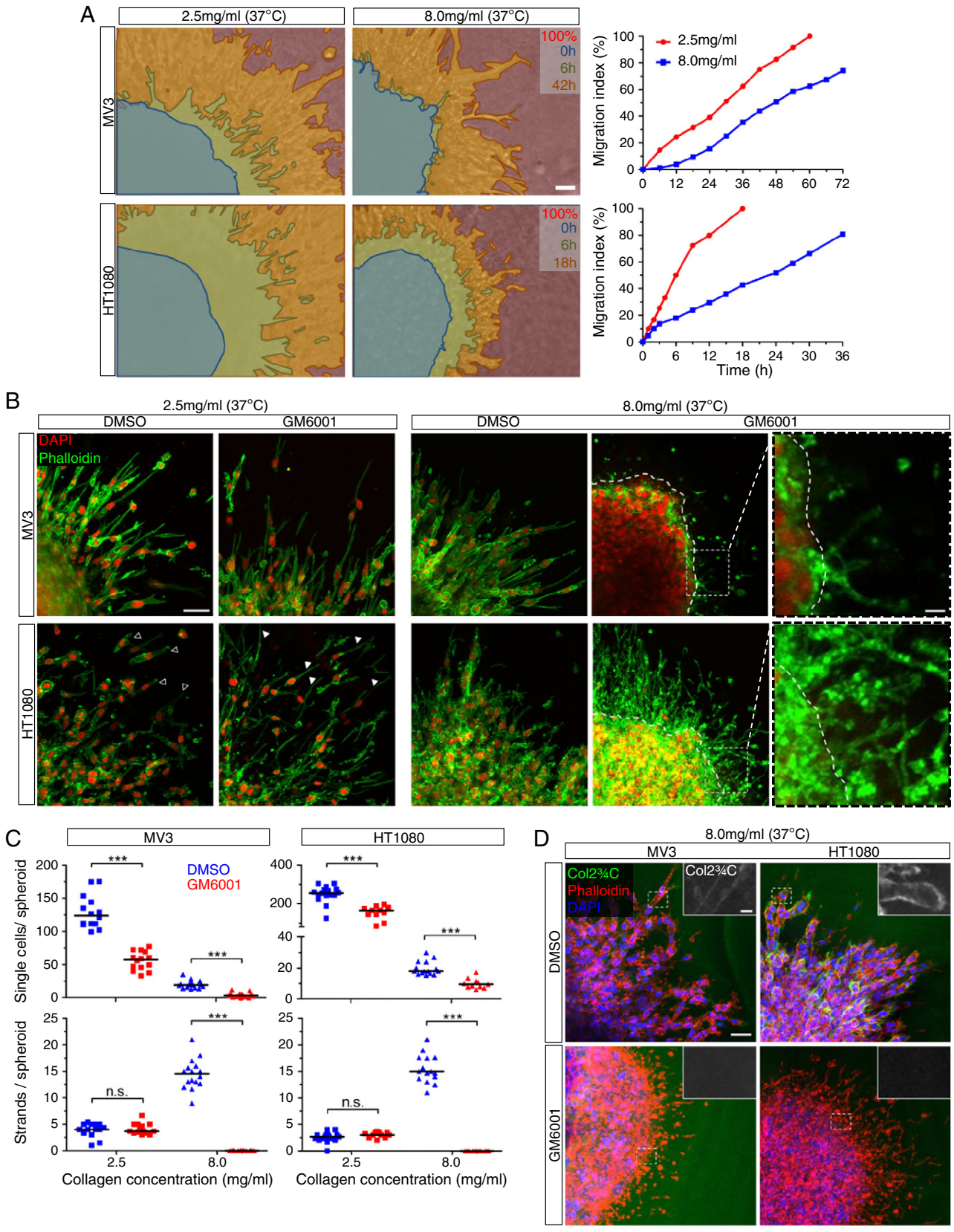

Fig. 3. Emigration delay of MV3 and HT1080 cells and proteolytic path clearance in dense ECM. A) Speed of emigration from spheroids embedded in collagen matrices of different densities. The migration index was calculated from frames taken at different time points from Movies #1 & 2 as the area covered with migrating cells minus initial spheroid area at 0 h (blue area). The 100% value corresponded to the maximum region covered by migrating cells at the end-point. B) Pattern and C) quantification of invasion efficiency of MV3 and HT1080 cells from spheroids treated with DMSO or MMP inhibitor GM6001. Black arrowheads: mesenchymal protrusions. White arrowheads: thin, filament-like protrusions. ***, $P < 0.0001$ and $P = 0.0002$ for HT1080 single cells 2.5 mg/ml DMSO vs. GM6001 and $P = 0.0007$ for HT1080 and MV3 strands 8.0 mg/ml DMSO vs. GM6001; ~30 spheroids/condition (3–4 independent experiments). D) Pericellular collagen degradation along invasion strands in dense collagen matrix. Differences in absolute Col2¾C signal intensity between both cell lines are caused by lower MMP-14 expression in MV3 compared to HT1080 cells (data not shown). Scale bars: 50 μm; 10 μm (insets B, D). Horizontal line: median.

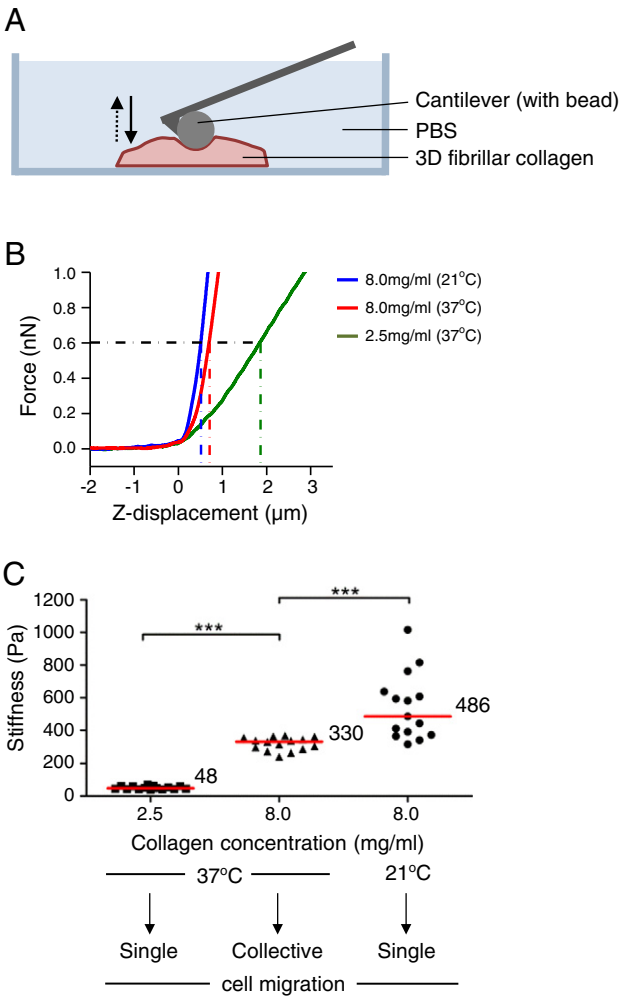

Fig. 4. Lack of correlation between invasion pattern and matrix stiffness. A) Principle of measuring collagen stiffness by atomic force microscopy (AFM). The cantilever was functionalized with a 10 μm bead to probe a 3D fibrillar collagen sample in PBS. B) Registration of Z-displacement while probing the surface of the collagen lattice by applying force with the bead-functionalized cantilever. The graph shows representative force curves of different collagen samples fitted with the Hertz deformation model. Dotted, vertical lines: deformation depth at 0.6 nN applied force. C) Stiffness for collagen matrices of different concentrations and polymerization conditions. ***, $P < 0.0001$; measurements at 10–15 different positions (average of 3 repetitive probing cycles per position) from 3 independent experiments. Red horizontal line: median.

and/or the dependence of cell translocation from protease engagement and proteolytic tissue remodeling [25,32]. Thereby, mesenchymal-to-amoeboid interconversion may represent a further response program to tissue-imposed confinement.

Multi-scale *in silico* computational modeling combining actomyosin dynamics and cell–matrix adhesion in the context of discontinuous or confined 3D matrix geometries retrieved no indication for the conversion from single-cell to collective migration of mesenchymal tumor cells [69]. A mechanically different monolayer-based *in silico* model combining cell density, amount of cell–cell adhesion and cell motility suggests the transition from individual-cell to sheet-like, collective movement as a function termed cell jamming phase diagram [48]. In this model, cell monolayers lack the stringent space confinement present in ECM-based 3D environments, however with increasing density ("jamming") cells gain cell–cell coordination during migration, thus representing a 2D variant of the here described matrix-density induced switch from single-cell to collective migration. In 3D environments, cell jamming occurs when space is limited and cells become increasingly confined, either in preexisting tissue tracks observed *in vivo* [16,17] or proteolytic *de novo* tracks generated by leader cells [1,8], which both provide space that approximates the width of single cells or small cell groups [23,26]. Because in high-density collagen lattices the pore cross-sections of the substrate and likely the boundaries of proteolytic tracks range below the physical limit of cell deformation (below 5–10 μm^2) [31], its inner lumen enables the jamming of follower cells which rather follow the track lining than breaking out laterally and establish new tracks.

The consequences of cell jamming on molecular cell functions, including cell-to-cell signaling and the molecular migration machinery, remain to be addressed. Mesenchymal tumor cells retain rather weak constitutive cell–cell adhesion, as indicated by spontaneous single cell dispersion in unconfined matrix conditions. However, cell jamming may impose contact-mediated secondary cell-to-cell signaling, altered protein-expression, -function and -localization, and eventually reinforce cell–cell junctions. In other mesenchymal cell models, cell–cell adhesion depends upon N-cadherin or adhesion receptors of the immunoglobulin family, including L1-CAM, NCAM, ALCAM, which may cooperate for multicellular interactivity and function [7,9,19,70,71]. Alternatively, in the absence of cell–cell adhesion engagement, confinement-imposed jamming may result in physical convolution of cell bodies which, despite high cell–cell proximity, maintain independent cytoskeletal activity and migrate as individual cells similar to multicellular streaming [2,5]. In other, microchannel-based models of cell migration, confined space causes a switch in molecular migration mechanisms, from actin-based kinetics to microtubule- or water-flux based, hydrostatic mechanisms of cell propulsion and transport [72,73]. Consequently, together with altered biomechanics, the impact of cell jamming on active *versus* passive cell–cell cooperation and, possibly, functionally inert, "agnostic" next-neighbor behaviors, will help to define subtypes of multicellular migration and associated cell-function states during migration in complex tissue.

5. Conclusions

These findings support the notion that mesenchymal cells with constitutively loose cell–cell adhesions [63,74,75] respond to ECM density by adjusting their cell–cell interactions, aggregation and protease dependence, and thereby transit from single-cell to collective invasion strategies, and vice versa. This plasticity response, albeit imposed by a physical mechanism that forces moving cells into and along confined tissue tracks, likely impacts the signals received from local cues, including organization of cell–matrix and cell–cell junctions. Future work will show whether the ECM-density induced collective pattern further induces cell–cell coupling by connexins, and altered signaling states, *e.g.* epithelium-like cell–cell junctions and apicobasal polarity reminiscent of MET[6] [9,10,75,76] and clarify the relevance of cell jamming in physiological and pathological contexts.

Supplementary data to this article can be found online at http://dx.doi.org/10.1016/j.bbagen.2014.03.020.

Acknowledgements

We gratefully acknowledge Joost te Riet (Department of Tumor Immunology, RIMLS, The Netherlands) for providing anti-ALCAM antibody. Work of AH was supported by the PhD fellowship program of the RadboudUMC (Nijmegen, The Netherlands). We further acknowledge support by the NWO-Vidi (917.10.364) to KW and by the European Research Council (617430-DEEPINSIGHT), NWO-Vici (918.11.626) and the Cancer Genomics Center (www.cancergenomics.nl) to PF. AFM work was supported by NWO Medium Sized Investment (NWO-ZonMW 91110007).

[6] Mesenchymal–epithelial transition.

References

[1] K. Wolf, Y.I. Wu, Y. Liu, J. Geiger, E. Tam, C. Overall, et al., Multi-step pericellular proteolysis controls the transition from individual to collective cancer cell invasion, Nat. Cell Biol. 9 (2007) 893–904.
[2] P. Friedl, S. Alexander, Cancer invasion and the microenvironment: plasticity and reciprocity, Cell 147 (2011) 992–1009.
[3] T. Lämmermann, M. Sixt, Mechanical modes of "amoeboid" cell migration, Curr. Opin. Cell Biol. 21 (2009) 636–644.
[4] P. Rørth, Fellow travellers: emergent properties of collective cell migration, EMBO Rep. 13 (2012) 984–991.
[5] P. Friedl, J. Locker, E. Sahai, J.E. Segall, Classifying collective cancer cell invasion, Nat. Cell Biol. 14 (2012) 777–783.
[6] X. Trepat, J.J. Fredberg, Plithotaxis and emergent dynamics in collective cellular migration, Trends Cell Biol. 21 (2011) 638–646.
[7] Y. Hegerfeldt, M. Tusch, E.B. Bröcker, P. Friedl, Collective cell movement in primary melanoma explants: plasticity of cell–cell interaction, Beta1-integrin function, and migration strategies, Cancer Res. 62 (2002) 2125–2130.
[8] C. Gaggioli, S. Hooper, C. Hidalgo-Carcedo, R. Grosse, J.F. Marshall, K. Harrington, et al., Fibroblast-led collective invasion of carcinoma cells with differing roles for RhoGTPases in leading and following cells, Nat. Cell Biol. 9 (2007) 1392–1400.
[9] P. Friedl, D. Gilmour, Collective cell migration in morphogenesis, regeneration and cancer, Nat. Rev. Mol. Cell Biol. 10 (2009) 445–457.
[10] M.A. Nieto, Epithelial plasticity: a common theme in embryonic and cancer cells, Science 342 (2013) 1234850.
[11] A. Gheldof, G. Berx, Cadherins and epithelial-to-mesenchymal transition, Prog. Mol. Biol. Transl. Sci. 116 (2013) 317–336.
[12] K. Maaser, K. Wolf, C.E. Klein, B. Niggemann, K.S. Zänker, E.B. Bröcker, et al., Functional hierarchy of simultaneously expressed adhesion receptors: integrin alpha2beta1 but not CD44 mediates MV3 melanoma cell migration and matrix reorganization within three-dimensional hyaluronan-containing collagen matrices, Mol. Biol. Cell 10 (1999) 3067–3079.
[13] K. Wolf, I. Mazo, H. Leung, K. Engelke, U.H. von Andrian, E.I. Deryugina, et al., Compensation mechanism in tumor cell migration: mesenchymal–amoeboid transition after blocking of pericellular proteolysis, J. Cell Biol. 160 (2003) 267–277.
[14] J. Bonaventure, M.J. Domingues, L. Larue, Cellular and molecular mechanisms controlling the migration of melanocytes and melanoma cells, Pigment Cell Melanoma Res. 26 (2013) 316–325.
[15] E. Theveneau, R. Mayor, Cadherins in collective cell migration of mesenchymal cells, Curr. Opin. Cell Biol. 24 (2012) 677–684.
[16] S. Alexander, G.E. Koehl, M. Hirschberg, E.K. Geissler, P. Friedl, Dynamic imaging of cancer growth and invasion: a modified skin-fold chamber model, Histochem. Cell Biol. 130 (2008) 1147–1154.
[17] B. Weigelin, G.-J. Bakker, P. Friedl, Intravital third harmonic generation microscopy of collective melanoma cell invasion: principles of interface guidance and microvesicle dynamics, Intra Vital 1 (2012) 32–43.
[18] M. Miron-Mendoza, X. Lin, L. Ma, P. Ririe, W.M. Petroll, Individual versus collective fibroblast spreading and migration: regulation by matrix composition in 3D culture, Exp. Eye Res. 99 (2012) 36–44.
[19] W. Shih, S. Yamada, N-cadherin-mediated cell–cell adhesion promotes cell migration in a three-dimensional matrix, J. Cell Sci. 125 (2012) 3661–3670.
[20] K. Wolf, P. Friedl, Extracellular matrix determinants of proteolytic and non-proteolytic cell migration, Trends Cell Biol. 21 (2011) 736–744.
[21] M.A. Karsdal, M.J. Nielsen, J.M. Sand, K. Henriksen, F. Genovese, A.-C. Bay-Jensen, et al., Extracellular matrix remodeling: the common denominator in connective tissue diseases. Possibilities for evaluation and current understanding of the matrix as more than a passive architecture, but a key player in tissue failure, Assay Drug Dev. Technol. 11 (2013) 70–92.
[22] C.M. Kraning-Rush, C.A. Reinhart-King, Controlling matrix stiffness and topography for the study of tumor cell migration, Cell Adh. Migr. 6 (2012) 274–279.
[23] K. Wolf, S. Alexander, V. Schacht, L.M. Coussens, U.H. von Andrian, J. van Rheenen, et al., Collagen-based cell migration models in vitro and in vivo, Semin. Cell Dev. Biol. 20 (2009) 931–941.
[24] P.P. Provenzano, D.R. Inman, K.W. Eliceiri, J.G. Knittel, L. Yan, C.T. Rueden, et al., Collagen density promotes mammary tumor initiation and progression, BMC Med. 6 (2008) 11.
[25] P. Friedl, K. Wolf, Plasticity of cell migration: a multiscale tuning model, J. Cell Biol. 188 (2010) 11–19.
[26] O. Ilina, G.-J. Bakker, A. Vasaturo, R.M. Hofmann, P. Friedl, Two-photon laser-generated microtracks in 3D collagen lattices: principles of MMP-dependent and -independent collective cancer cell invasion, Phys. Biol. 8 (2011) 015010.
[27] C.M. Nelson, M.J. Bissell, Of extracellular matrix, scaffolds, and signaling: tissue architecture regulates development, homeostasis, and cancer, Annu. Rev. Cell Dev. Biol. 22 (2006) 287–309.
[28] C. Londono, M.J. Loureiro, B. Slater, P.B. Lucker, J. Soleas, S. Sathananthan, et al., Nonautonomous contact guidance signaling during collective cell migration, Proc. Natl. Acad. Sci. 111 (2014) 1807–1812.
[29] F. Bordeleau, L.N. Tang, C.A. Reinhart-King, Topographical guidance of 3D tumor cell migration at an interface of collagen densities, Phys. Biol. 10 (2013) 065004.
[30] P.P. Provenzano, D.R. Inman, K.W. Eliceiri, S.M. Trier, P.J. Keely, Contact guidance mediated three-dimensional cell migration is regulated by Rho/ROCK-dependent matrix reorganization, Biophys. J. 95 (2008) 5374–5384.
[31] K. Wolf, M. Te Lindert, M. Krause, S. Alexander, J. Te Riet, A.L. Willis, et al., Physical limits of cell migration: control by ECM space and nuclear deformation and tuning by proteolysis and traction force, J. Cell Biol. 201 (2013) 1069–1084.
[32] K. Wolf, R. Müller, S. Borgmann, E.-B. Bröcker, P. Friedl, Amoeboid shape change and contact guidance: T-lymphocyte crawling through fibrillar collagen is independent of matrix remodeling by MMPs and other proteases, Blood 102 (2003) 3262–3269.
[33] S.D. Mason, J.A. Joyce, Proteolytic networks in cancer, Trends Cell Biol. 21 (2011) 228–237.
[34] F. Sabeh, X.-Y. Li, T.L. Saunders, R.G. Rowe, S.J. Weiss, Secreted versus membrane-anchored collagenases: relative roles in fibroblast-dependent collagenolysis and invasion, J. Biol. Chem. 284 (2009) 23001–23011.
[35] P. Friedl, K. Wolf, Tube travel: the role of proteases in individual and collective cancer cell invasion, Cancer Res. 68 (2008) 7247–7249.
[36] M. Miron-Mendoza, J. Seemann, F. Grinnell, The differential regulation of cell motile activity through matrix stiffness and porosity in three dimensional collagen matrices, Biomaterials 31 (2010) 6425–6435.
[37] R.J. Pelham, Y. Wang, l. Cell locomotion and focal adhesions are regulated by substrate flexibility, Proc. Natl. Acad. Sci. U. S. A. 94 (1997) 13661–13665.
[38] P. Vitorino, T. Meyer, Modular control of endothelial sheet migration, Genes Dev. 22 (2008) 3268–3281.
[39] S. Rasheed, W.A. Nelson-Rees, E.M. Toth, P. Arnstein, M.B. Gardner, Characterization of a newly derived human sarcoma cell line (HT-1080), Cancer 33 (1974) 1027–1033.
[40] G.N. Van Muijen, K.F. Jansen, I.M. Cornelissen, D.F. Smeets, J.L. Beck, D.J. Ruiter, Establishment and characterization of a human melanoma cell line (MV3) which is highly metastatic in nude mice, Int. J. Cancer 48 (1991) 85–91.
[41] D. Del Duca, T. Werbowetski, R.F. Del Maestro, Spheroid preparation from hanging drops: characterization of a model of brain tumor invasion, J. Neuro-Oncol. 67 (2004) 295–303.
[42] J. Schindelin, I. Arganda-Carreras, E. Frise, V. Kaynig, M. Longair, T. Pietzsch, et al., Fiji: an open-source platform for biological-image analysis, Nat. Methods 9 (2012) 676–682.
[43] J.M.D.T. Nelissen, I.M. Peters, B.G. de Grooth, Y. van Kooyk, C.G. Figdor, Dynamic regulation of activated leukocyte cell adhesion molecule-mediated homotypic cell adhesion through the actin cytoskeleton, Mol. Biol. Cell 11 (2000) 2057–2068.
[44] M. Krause, J. te Riet, K. Wolf, Probing the compressibility of tumor cell nuclei by combined atomic force–confocal microscopy, Phys. Biol. 10 (2013) 065002.
[45] D.C. Lin, E.K. Dimitriadis, F. Horkay, Robust strategies for automated AFM force curve analysis—I. Non-adhesive indentation of soft, inhomogeneous materials, J. Biomech. Eng. 129 (2007) 430–440.
[46] P. Friedl, K. Maaser, C.E. Klein, B. Niggemann, G. Krohne, K.S. Zänker, Migration of highly aggressive MV3 melanoma cells in 3-dimensional collagen lattices results in local matrix reorganization and shedding of alpha2 and beta1 integrins and CD44, Cancer Res. 57 (1997) 2061–2070.
[47] A. Pathak, S. Kumar, Independent regulation of tumor cell migration by matrix stiffness and confinement, Proc. Natl. Acad. Sci. U. S. A. 109 (2012) 10334–10339.
[48] M. Sadati, N. Taheri Qazvini, R. Krishnan, C.Y. Park, J.J. Fredberg, Collective migration and cell jamming, Differentiation 86 (2013) 121–125.
[49] P. Stoitzner, K. Pfaller, H. Stössel, N. Romani, A close-up view of migrating Langerhans cells in the skin, J. Investig. Dermatol. 118 (2002) 117–125.
[50] D.T. Butcher, T. Alliston, V.M. Weaver, A tense situation: forcing tumour progression, Nat. Rev. Cancer 9 (2009) 108–122.
[51] A. Buxboim, I.L. Ivanovska, D.E. Discher, Matrix elasticity, cytoskeletal forces and physics of the nucleus: how deeply do cells "feel" outside and in? J. Cell Sci. 123 (2010) 297–308.
[52] A.M. Stein, D.A. Vader, L.M. Jawerth, D.A. Weitz, L.M. Sander, An algorithm for extracting the network geometry of three-dimensional collagen gels, J. Microsc. 232 (2008) 463–475.
[53] K.R. Levental, H. Yu, L. Kass, J.N. Lakins, M. Egeblad, J.T. Erler, et al., Matrix crosslinking forces tumor progression by enhancing integrin signaling, Cell 139 (2009) 891–906.
[54] Z. Tong, E.M. Balzer, M.R. Dallas, W.-C. Hung, K.J. Stebe, K. Konstantopoulos, Chemotaxis of cell populations through confined spaces at single-cell resolution, PLoS One 7 (2012) e29211.
[55] E.M. Balzer, Z. Tong, C.D. Paul, W.-C. Hung, K.M. Stroka, A.E. Boggs, et al., Physical confinement alters tumor cell adhesion and migration phenotypes, FASEB J. 26 (2012) 4045–4056.
[56] W.-C. Hung, S.-H. Chen, C.D. Paul, K.M. Stroka, Y.-C. Lo, J.T. Yang, et al., Distinct signaling mechanisms regulate migration in unconfined versus confined spaces, J. Cell Biol. 202 (2013) 807–824.
[57] R. Xu, A. Boudreau, M.J. Bissell, Tissue architecture and function: dynamic reciprocity via extra- and intra-cellular matrices, Cancer Metastasis Rev. 28 (2009) 167–176.
[58] P.G. Gritsenko, O. Ilina, P. Friedl, Interstitial guidance of cancer invasion, J. Pathol. 226 (2012) 185–199.
[59] K.-V. Nguyen-Ngoc, K.J. Cheung, A. Brenot, E.R. Shamir, R.S. Gray, W.C. Hines, et al., ECM microenvironment regulates collective migration and local dissemination in normal and malignant mammary epithelium, Proc. Natl. Acad. Sci. U. S. A. 109 (2012) E2595–E2604.
[60] P. Friedl, P.B. Noble, P.A. Walton, D.W. Laird, P.J. Chauvin, R.J. Tabah, et al., Migration of coordinated cell clusters in mesenchymal and epithelial cancer explants in vitro, Cancer Res. 55 (1995) 4557–4560.
[61] R.S. Gray, K.J. Cheung, A.J. Ewald, Cellular mechanisms regulating epithelial morphogenesis and cancer invasion, Curr. Opin. Cell Biol. 22 (2010) 640–650.
[62] J.J. Christiansen, A.K. Rajasekaran, Reassessing epithelial to mesenchymal transition as a prerequisite for carcinoma invasion and metastasis, Cancer Res. 66 (2006) 8319–8326.
[63] M.L. Wynn, P. Rupp, P.A. Trainor, S. Schnell, P.M. Kulesa, Follow-the-leader cell migration requires biased cell–cell contact and local microenvironmental signals, Phys. Biol. 10 (2013) 035003.

[64] E. Theveneau, B. Steventon, E. Scarpa, S. Garcia, X. Trepat, A. Streit, et al., Chase-and-run between adjacent cell populations promotes directional collective migration, Nat. Cell Biol. 15 (2013) 763–772.
[65] E. Theveneau, R. Mayor, Neural crest delamination and migration: from epithelium-to-mesenchyme transition to collective cell migration, Dev. Biol. 366 (2012) 34–54.
[66] E. Theveneau, R. Mayor, Can mesenchymal cells undergo collective cell migration? The case of the neural crest. Cell Adh. Migr. 5 (2011) 490–498.
[67] P.H. Strobl-Mazzulla, M.E. Bronner, Epithelial to mesenchymal transition: new and old insights from the classical neural crest model, Semin. Cancer Biol. 22 (2012) 411–416.
[68] A.A. Khalil, P. Friedl, Determinants of leader cells in collective cell migration, Integr. Biol. (Camb.) 2 (2010) 568–574.
[69] M. Tozluoğlu, A.L. Tournier, R.P. Jenkins, S. Hooper, P. Bates, E. Sahai, Matrix geometry determines optimal cancer cell migration strategy and modulates response to interventions, Nat. Cell Biol. 15 (2013) 751–762.
[70] W. Shih, S. Yamada, N-cadherin as a key regulator of collective cell migration in a 3D environment, Cell Adh. Migr. 6 (2012) 513–517.
[71] T. Kawauchi, Cell adhesion and its endocytic regulation in cell migration during neural development and cancer metastasis, Int. J. Mol. Sci. 13 (2012) 4564–4590.
[72] P.S. Raman, C.D. Paul, K.M. Stroka, K. Konstantopoulos, Probing cell traction forces in confined microenvironments, Lab Chip 13 (2013) 4599–4607.
[73] K.M. Stroka, H. Jiang, S.-H. Chen, Z. Tong, D. Wirtz, S.X. Sun, et al., Water permeation drives tumor cell migration in confined microenvironments, Cell 157 (2014) 1–13.
[74] B. Da Rocha-Azevedo, F. Grinnell, Fibroblast morphogenesis on 3D collagen matrices: the balance between cell clustering and cell migration, Exp. Cell Res. 319 (2013) 2440–2446.
[75] E. Theveneau, R. Mayor, Collective cell migration of epithelial and mesenchymal cells, Cell. Mol. Life Sci. 70 (2013) 3481–3492.
[76] O. Ilina, P. Friedl, Mechanisms of collective cell migration at a glance, J. Cell Sci. 122 (2009) 3203–3208.